Equilibrium states and ground state of two-dimensional fluid foams

F. Graner,[1,*] Y. Jiang,[2] E. Janiaud,[3] and C. Flament[3]

[1]*CNRS UMR 5588 et Université Grenoble I, Laboratoire de Spectrométrie Physique, Boîte Postale 87,*
F-38402 St. Martin d'Hères Cedex, France
[2]*Theoretical Division, Los Alamos National Laboratory, Los Alamos, New Mexico 87545*
[3]*Laboratoire des Milieux Désordonnés et Hétérogènes, case 78, Université Paris 6, Paris Cedex 05, France;*
CNRS UMR 7603, 4 place Jussieu, 75252 Paris Cedex 05, France;
and Université Paris 7, Denis Diderot, Unité de Formation et de Recherche de Physique (case 70.08), 2 place Jussieu,
75251 Paris Cedex 05, France

We study the equilibrium energies of two-dimensional (2D) noncoarsening fluid foams, which consist of bubbles with fixed areas. The equilibrium states correspond to local minima of the total perimeter. We present a theoretical derivation of energy minima; experiments with ferrofluid foams, which can be either highly distorted, locally relaxed, or globally annealed; and Monte Carlo simulations using the extended large-Q Potts model. For a dry foam with small size variance we develop physical insight and an electrostatic analogy, which enables us to (i) find an approximate value of the global minimum perimeter, accounting for (small) area disorder, the topological distribution, and physical boundary conditions; (ii) conjecture the corresponding pattern and topology: small bubbles sort inward and large bubbles sort outward, topological charges of the same signs "repel" while charges of the opposite signs "attract;" (iii) define local and global markers to determine directly from an image how far a foam is from its ground state; (iv) conjecture that, in a local perimeter minimum at prescribed topology, the pressure distribution and thus the edge curvature are unique. Some results also apply to 3D foams.

I. INTRODUCTION

Fluid foams or cellular fluids are a class of materials that consist of a collection of bubbles surrounded by a continuous phase which tends to minimize its surface energy under the volume constraint. The exact description of the ground state is a deep mathematical problem, while the characterization of all the metastable states provides insights into the physics of foams as well as industrial applications. Our motivations to study fluid foams are thus threefold.

For mathematicians, foams have long been an important tool to provide insights into the classic "isoperimetric problem": how to determine the minimal perimeter enclosing a cluster of N bubbles with known areas. Hales [1] recently proved the 2000-year-old honeycomb conjecture [2]: a cluster of two-dimensional (2D) bubbles of the same area reaches its minimum perimeter when all bubbles are regular hexagons. The conjecture is true only if the bubble cluster has no boundaries, i.e., the cluster is either infinite or has periodic boundary conditions. Besides this result, only the case $N=2$, i.e., the double-bubble problem, has been solved in 2D and 3D; $N=3$ and larger in 2D and higher dimensions have been partly studied [3–10]. Here we use the physics of equilibrium energy to find the perimeter "minimizer" in cases that have thus far escaped rigorous study, including large N, real boundary conditions, area, and topological disorder dispersity. We estimate the value of the perimeter minimum, and conjecture the corresponding patterns to be candidates for the minimizer. We hope to provide insight for future rigorous mathematical proofs.

For physicists, foams are a model for a class of materials that minimize surface energy: soap foams, emulsions, magnetic garnets, and even grain boundaries in polycrystals [11–17]. They share many common features of a cellular structure, including Plateau's rules (see below) and empirically observed topological and geometrical correlations [18]. Here we derive more general consequences of the energy minimization. Open questions we aim to answer include the following: Given an image of a foam can we determine whether the foam is stressed and deformed? How regular are bubble shapes at equilibrium? How do topology (number of neighbors of a bubble), pressure, and energy relate? What variables best describe the foam on a mesoscopic scale? Why do pentagons and heptagons tend to cluster in pairs in 2D foams?

More practically, understanding foams has technological importance. Industrial applications of foams, ranging from food and shaving cream to fire fighting and oil recovery [12,16,17], depend on their mechanical properties, which are not yet well understood. Foams support small stress like a solid, but flow under sufficiently large shear like a fluid, when the bubbles rearrange from one metastable configuration to another. This solidlike to fluidlike transition depends sensitively on the foam's structure [19]. Hence understanding foam structure is an important step toward predicting its mechanical properties, e.g., the quasistatic stress-strain relationship. Moreover, the structure of fluid foams determines the structure of solid foams produced by solidification, including: metallic foams in automobiles, pumice in volcanos, polymeric foams in filling materials, and food foams. Our present approach can potentially also provide a deeper un-

---

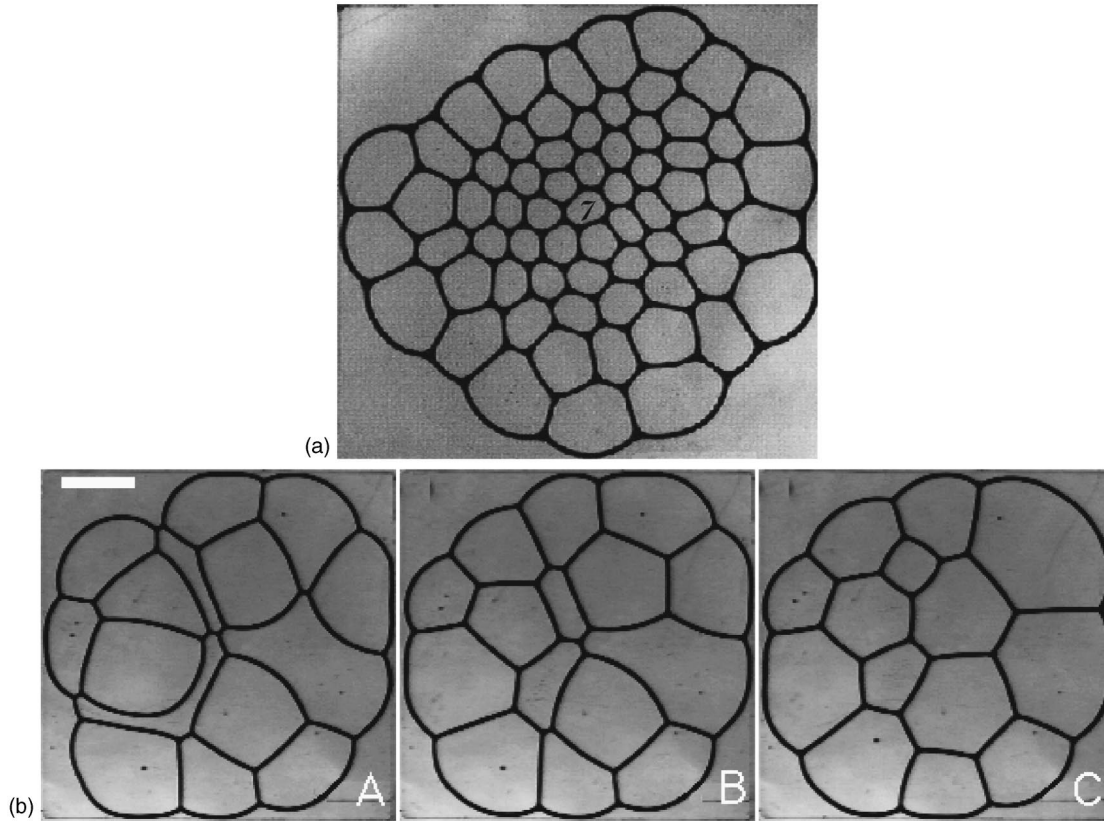*Corresponding author. Email address: graner@ujf-grenoble.fr

FIG. 1. Ferrofluid foams with fixed areas. (a) Annealed FFF image with free boundary, area dispersity $\delta A = 0.443\bar{A}$, and wall thickness $= 0.126\bar{A}^{1/2}$. The only heptagon is indicated by a number 7. See Sec. III A for preparation method. (b) A. Freshly formed FFF with highly distorted bubbles. B. The same foam after an avalanche of relaxational bubble rearrangements. C. The same after forcing a few bubble relaxations. Scale bar length is 20 mm.

derstanding of other more complex and heterogeneous materials which share one or more characteristics of fluid foam, e.g., dry and wet granular materials, aggregates of vesicles, biological cells, fracture patterns, and convection cells in aggregates.

Our starting point is two-dimensional noncoarsening foam. Such patterns result from surface energy minimization and capture the essence of any foam at a given time. Foams are almost always at quasiequilibrium because the bubble walls equilibrate on a very short time scale after a mechanical perturbation. The area distribution, of course, varies. However, the processes that cause area changes, such as coarsening, wall breakage, cell division, and cell nucleation, all act on a much slower time scale, and thus can be neglected in our current study of configuration energy. We hope our understanding of 2D foams will clarify 3D foams. We will indicate when our results apply to 3D.

We first present our theoretical, experimental, and numerical methods. Section II estimates the global energy minimum, and shows that experimental and simulated relaxed foams tend toward it. Sections III–V treat the energy of a real foam as perturbations around the ground state in the weak disorder limit: corrections from area disorder, topological disorder, and boundary conditions to the global minimum, respectively. Section VI summarizes the implications of our results.

A. Formulation

We use the word ''boundary'' as the external limit of a foam, and ''edge'' as the thin fluid line between two bubbles. For a foam with N bubbles with given areas $\{A_i, i = 1, \ldots, N\}$ [e.g., Fig. 1(a)], the energy of such a foam is simply the sum of edge lengths l_{ij} between bubbles i and j:

$$H = \gamma \sum_{0 \leq i < j \leq N} l_{ij}, \tag{1}$$

where $i = 0$ denotes the medium that surrounds the foam. Here γ, in J m^{-1}, is the energy cost of a unit line of a wall, the ''2D surface tension'' or ''line tension'' of the foam. In an experimental foam, an edge contains two interfaces between the edge fluid and the inner fluid. Equivalently, we can write

$$H = \frac{\gamma}{2} \sum_{i,j=0}^{N} l_{ij} = \frac{\gamma}{2} \sum_{i=0}^{N} \mathcal{L}_i, \tag{2}$$

where $l_{ii} = 0$, $\mathcal{L}_i = \Sigma_j l_{ij}$ is the perimeter of bubble i, and $\gamma/2$ is the usual surface tension between both fluids times the height of the bubble wall in the third dimension.

At equilibrium, i.e., in a local energy minimum, the foam obeys the Plateau rules (see [12,14,17] for physical explana-

tions and [4,5,7,8] for mathematical demonstrations): bubble edges are circular arcs that meet in triples at $2\pi/3$ angles [5]. According to Laplace's law their algebraic curvatures ($\kappa_{ij} = -\kappa_{ji} > 0$ when bubble i is convex compared with bubble j) are related to the 2D pressure P_i inside bubble i:

$$\kappa_{ij} = \frac{P_i - P_j}{\gamma}. \tag{3}$$

Thus the algebraic curvatures of the three edges that meet at the same vertex must add to zero [8]:

$$\kappa_{ij} + \kappa_{jk} + \kappa_{ki} = 0. \tag{4}$$

Equation (4) holds for any closed contour crossing more edges. It is also valid in 3D, with κ the mean curvature of a bubble face.

Mathematically, for a given foam consisting of N bubbles of fixed areas, finding the global minimum (ground state) and local minima (equilibrium states) of the foam energy H is equivalent to minimizing the sum of all bubble perimeters. In this sense, the problem is purely geometrical. The surface tension and average bubble area $\bar{A}$ scale out; the details of the foam enter only through the distribution normalized areas $A_i/\bar{A}$. Moreover, if we draw a path from bubble 1 to bubble i, the sum of the curvatures of all edges crossed determines P_i/γ directly from the foam's image, up to an additive constant P_1/γ; Eq. (4) ensures that the resulting measurement of P/γ is unique. The problem is the same for *any* foam, and more generally for any perimeter minimization, even if H is not proportional to the perimeter [20].

In the same spirit, we make the following assumptions (which we can relax later).

(1) We assume that each bubble encloses a fixed mass, which relates its area to its pressure. We further assume incompressibility; thus each bubble's area is constant.

(2) We consider only isotropic surface tensions. Most real foams require corrections: microscopic or long-range interactions, external force fields, or surface tension anisotropy. We do not consider the Marangoni variations of surface tension.

(3) If the continuous phase occupies a fraction ϕ of the foam, the mathematical ideal case corresponds to $\phi = 0$ while actual materials have a finite ϕ. We assume the "dry foam" limit $\phi \ll 1$. We assume that the thickness of the bubble walls is uniform throughout the foam and scales like ϕ. We neglect drainage and Plateau borders. This restriction makes sense because all physically relevant quantities have a regular limit when ϕ tends to 0.

(4) In a perfectly ordered foam, i.e., the honeycomb structure, all bubbles are hexagons with the same area. For reasons that will soon become clear, we consider weakly disordered foams "close to a honeycomb structure," where both the area and the edge number distributions have small variances. Despite their weak disorder, such foams may lack long-range orientational and translational order and thus may be homogeneous and isotropic on large scales. We do not consider infinite foams, which can have an infinite variance of area distribution.

B. Experiments

As an experimental model, we choose ferrofluid foams (FFF's), which we can easily manipulate to produce large distortions or to force relaxations. Good image contrast, centimeter length scales, and few second local relaxation times facilitate observations.

A detailed description of FFF's has appeared in [21]. A FFF is an immiscible mixture of an ionic magnetic fluid (aqueous black magnetic liquid) and oil (white spirit) in fractions ranging from 7%-93% to 13%-87%. The fluid mixture is trapped in the 1 mm space between two parallel 10×10 cm^2 Plexiglas plates. A homogeneous magnetic field of 9 kA/m perpendicular to the plates induces the cellular structure and fixes the bubble edge thickness. Figure 1 shows an equilibrium FFF picture; the magnetic fluid forms dark lines. We measure areas directly from the images and edge lengths from skeletonized images (foam edges shrunk to lines with single pixels). The same oil as that filling the bubbles surrounds them. Preparation conditions fix the bubble areas, which vary very slowly (time scale $\sim 10^4$ s in an ac field, $>10^6$ s in a dc field).

A FFF behaves like a 2D soap foam [22]. For an oil-water surface tension of 15 mN/m and a bubble size of 1 cm, as in Fig. 1, the magnetic dipolar interaction energy and the thermal energy $k_B T$ are $\approx 2\%$ and $\approx 10^{-16}$ of the surface tension times a bubble diameter, respectively. As a consequence, the FFF obeys the Plateau rules.

C. Simulations

We use the extended large-Q Potts model, which allows large numbers of bubbles, $N \gg 1$, no fluid fraction $\phi = 0$, fixed bubble areas, a large range of area distributions, and large foam distortions [19] [Fig. 2(a)]. The foam is simulated at zero temperature and bubble edges relax quickly upon perturbation; i.e., the foam is almost always at equilibrium, like soap froth.

The model treats a foam on a 2D lattice by assigning an integer index to each lattice site. Domains of like index are bubbles. Each pair of neighbors having unmatching indices determines a bubble wall and contributes to the bubble wall surface energy. Thus energy minimization through Monte Carlo dynamics minimizes bubble perimeters. Bubble areas are the number of lattice sites for each index; an area constraint keeps the bubble areas constant. To ensure that surface tension and measurements are isotropic and insensitive to the lattice [23], the energy for the Monte Carlo evolution is evaluated with fourth nearest neighbor interactions. The edge lengths and perimeters are determined using the weighted second nearest neighbors: $l = (\sqrt{2} - 1)N_1 + (1 - 1/\sqrt{2})N_2$, with N_1 and N_2 the number of nearest neighbors and next nearest neighbors at the edge, respectively. This method overestimates the edge length at most by $1/N$, N being the number of lattice sites at an edge. Thus the error is less than a few percent in the simulations presented here.

II. ZEROTH-ORDER ESTIMATE OF THE GLOBAL MINIMUM

A. Lower bound H_h

If all the bubble areas A_i are known but their topology is free to vary, a minimum value min(H) for the foam energy
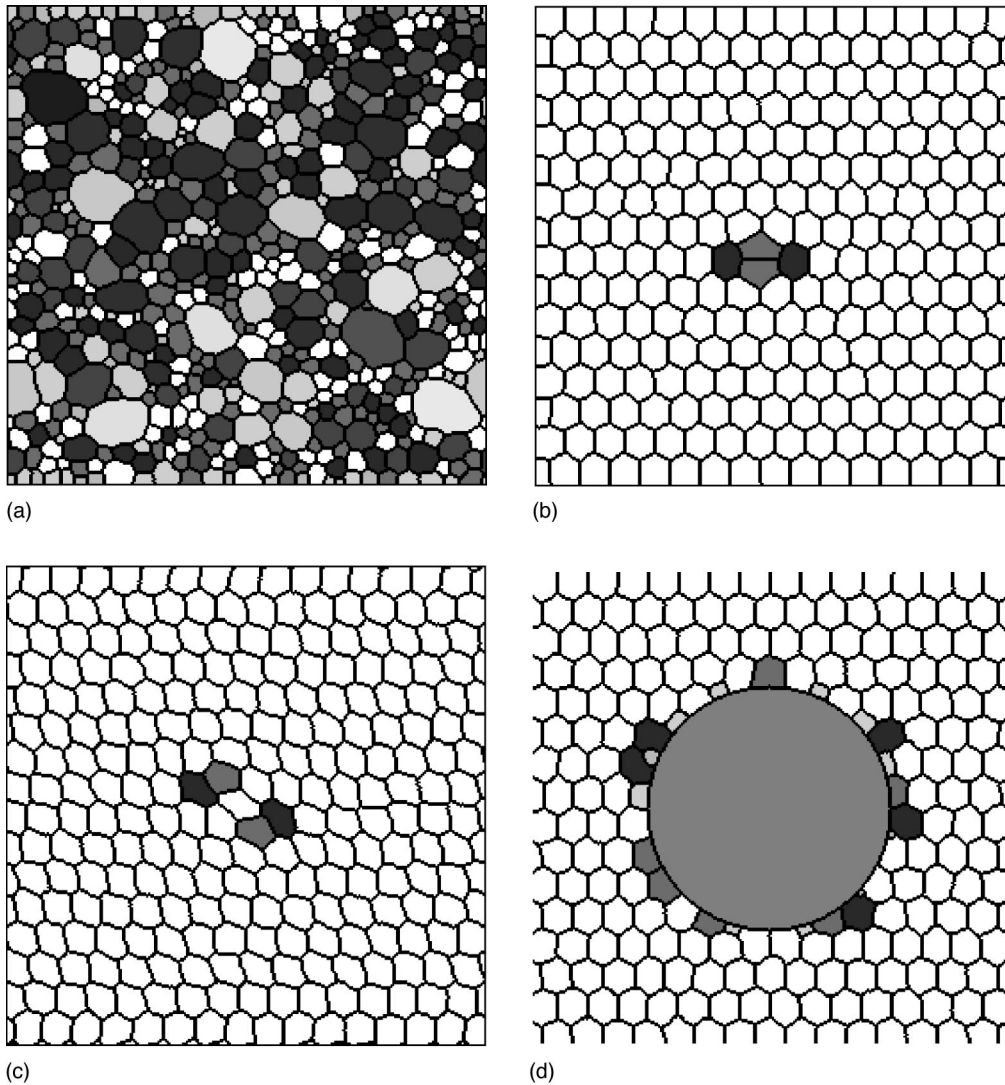
FIG. 2. Simulated foams with fixed areas. (a) A typical configuration of a polydispersed foam at equilibrium. The top and bottom boundaries are fixed, the lateral boundaries periodic. The lattice is 256×256 with 589 bubbles. Shades of gray encode the number of neighbors each bubble has. The area dispersity is $\delta A / \bar{A} = 1.06$. (b) A regular foam with equal areas ($\delta A / \bar{A} = 0.4\%$) and periodic boundaries. An artificially constructed pentagon-heptagon-pentagon-heptagon cluster forms a topological quadrupole, with the rest of the honeycomb lattice undisturbed. (c) Two dipoles (pentagon-heptagon pairs) result in a curvature field in the hexagons around them. (d) A foam illustrating the fixed boundary conditions: a circular obstacle in the center of a hexagonal foam induces a topological charge distribution in the bubbles touching its boundary; all the edges are perpendicular to the solid boundary.

(i.e., the ground state) exists [4]. However, its value, and the corresponding pattern(s), is an open problem. Both the following conjectures are discussed in the Appendix:
(1) min(H) admits a simple lower bound:

$$\min(H) \geqslant 3.71 \frac{\gamma}{2} \sum_{i=1}^{N} \sqrt{A_i}. \quad (5)$$

(2) The energy of a natural, polydisperse, random foam is at least the energy of a collection of regular hexagons with the same areas. Equivalently, min(H) admits a zeroth-order estimate H_h:

$$H_h \sim 3.72 \frac{\gamma}{2} \sum_{i=1}^{N} \sqrt{A_i}. \quad (6)$$

min(H) is close to, but larger than H_h. This estimate of the global minimum H_h depends on only the area distribution, not the pattern. Thus, given an image, we can simultaneously measure H, through the actual edge lengths, and H_h, through the areas. The ratio H/H_h is a global marker of the energy stored in the foam, or how far the foam is from its global minimum at prescribed areas. We will now examine this ratio in FFF experiments and simulations.

B. Applications of H_h

In FFF experiments, a metallic pin, when placed above the FFF, locally channels the magnetic field lines and attracts some ferrofluid. This enables us to locally perturb the vertices [22]. We use this magnetic manipulation to prepare five
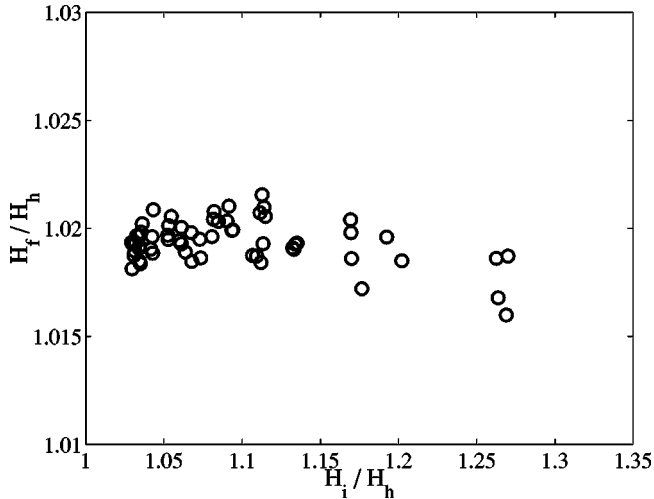
FIG. 3. Relaxed energy of a random foam [Fig. 2(a)]. The final rescaled equilibrium energies H_f/H_h after long relaxations (10^6 Monte Carlo steps MCS) are plotted against the initial energy H_i/H_h. Note the difference in horizontal and vertical scales.

FIG. 4. Relaxation of FFF's: Standard deviation $\delta(l_{ij}/L_{ij})$ as a function of rescaled energy H/H_h. The five different symbols (circles, triangles, squares, diamonds, and pentagons) correspond to five relaxation experiments similar to the process shown in Fig. 1(b). Highly distorted foams (initial foams in open symbols) relax through avalanches of T1 processes (partially relaxed foams in gray symbols), and magnetic manipulations (completely relaxed foams in closed symbols).

different foams with highly distorted bubbles [Fig. 1(b)]. The foams then spontaneously relax via an avalanche of neighbor-switching events (or topological rearrangements, often termed *T1 processes*), their energies relax to a value slightly higher than H_h. By displacing each vertex one by one, we force all the T1 processes we can [22] to produce more regular bubbles: the energy decreases even closer to H_h (data shown in the abscissa of Fig. 4).

In the extended Potts model, by biasing the Monte Carlo lattice upate, we can apply a steady shear [19] to prepare a distorted foam: a higher shear rate results in more distorted bubbles, and thus higher initial energy. We let the distorted foams relax toward equilibrium, i.e., a local energy minimum. Figure 3 shows that, whatever their initial energy, the relaxed foams all have final energies 2% above H_h. Initially more distorted foams seem to reach a final energy closer to H_h.

We now write the energy of the foam as H_h plus three corrections:

$$H = H_h + H_a + H_t + H_b, \tag{7}$$

where the subscripts stand, respectively, for hexagons, area disorder, topological defects, and boundaries. For simplicity, we want to treat these corrections separately, as perturbations around the ground state H_h. This applies to weakly disordered foams with small area and topology variations.

III. AREA DISORDER

A. Minimization of area mismatch

The edges of a regular hexagon of area A have length $L = 3.72\sqrt{A}/6$ [24]. If two bubbles of different areas $A_i > A_j$ share a common edge, its length l_{ij} obviously cannot be simultaneously equal to both L_i and L_j. There is thus an energy cost associated with the area mismatch, $\epsilon = (A_i - A_j)/(A_i + A_j)$, which vanishes only for $\epsilon = 0$. For small
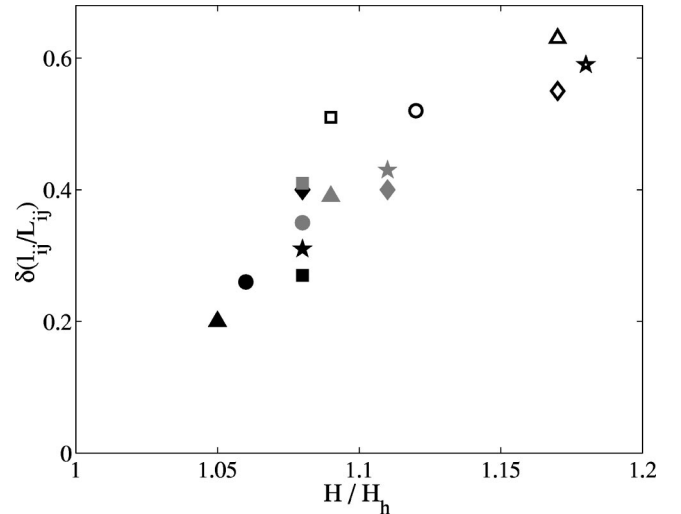
area mismatch $\epsilon \ll 1$, and for bubbles far from the foam boundaries, each edge contribution to H_a is quadratic in ϵ, i.e., proportional to $\sim \gamma \epsilon^2$ (the strain energy [25]).

If the area disorder is small enough, the foam reduces its energy when the topological disorder is also small [26]. When each bubble is surrounded by neighbors of nearly the same area and reaches a nearly regular shape, i.e., when bubbles sort according to their sizes, the energy minimum is reached. Most bubbles are hexagons and form a slightly distorted honeycomb lattice. H_a then corresponds to the strain energy in growing a crystal with increasing lattice size [25]. For a foam with free boundaries and no external force field, we expect the bubbles to sort according to their sizes; and the smaller ones inward, the larger ones outward, as in crystals [25].

This is exactly what we observe in ''annealed'' FFF's. We tilt the Plexiglas plates from the horizontal plane to an angle of $0.1\,°$, inducing a low effective gravity field. Large bubbles drift upward, small bubbles downward, resulting in vertical sorting according to size. We can achieve the same result with a magnetic gradient [27]. We then bring the plates back to horizontal, and the bubbles slowly drift and settle. This procedure allows the bubbles to rearrange and explore the energy space to find a lower energy configuration. The final stable pattern [Fig. 1(a)] displays round bubbles and radial sorting according to size, larger bubbles surrounding smaller ones. Coming closer to the ground state would require individual bubble manipulations. We expect that the same size sorting should occur in 3D foams as well.

B. Optimal edge length

The actual value of l_{ij} results from a minimization over the whole foam including the boundary conditions, which is

(a)

FIG. 6. Different equilibrated foams. Each foam is simulated with periodic boundaries. They have the same topology, but different area polydispersity and hence different energy ratios H/H_h. Average $\langle l_{ij}/L_{ij} \rangle \sim 1$ (circles, left ordinate) and standard deviation $\delta(l_{ij}/L_{ij}) \ll 1$ (stars, right ordinate) indicate that each l_{ij} is close to L_{ij}.

the compression tend to be smaller than their L_{ij}. Thus the average $\langle l_{ij}/L_{ij} \rangle$ and the variance $\delta(l_{ij}/L_{ij})$ intrinsically define a foam's strain [28,29].

To estimate L_{ij}, if we stay close to a honeycomb lattice, we require that L_{ij} depends on A_i and A_j only, and is symmetric in A_i, A_j. L_{ij} likely lies between L_i and L_j and, in order to locally minimize the perimeter under the area constraints, L_{ij} should be smaller than $(L_i + L_j)/2$. The geometrical average is one of the most natural candidates:

$$L_{ij} \equiv \sqrt{L_i L_j} = \frac{3.72}{6} (A_i A_j)^{1/4}, \tag{8}$$

which we can test by measuring the distribution of l_{ij}/L_{ij} in both FFF's and simulated foams.
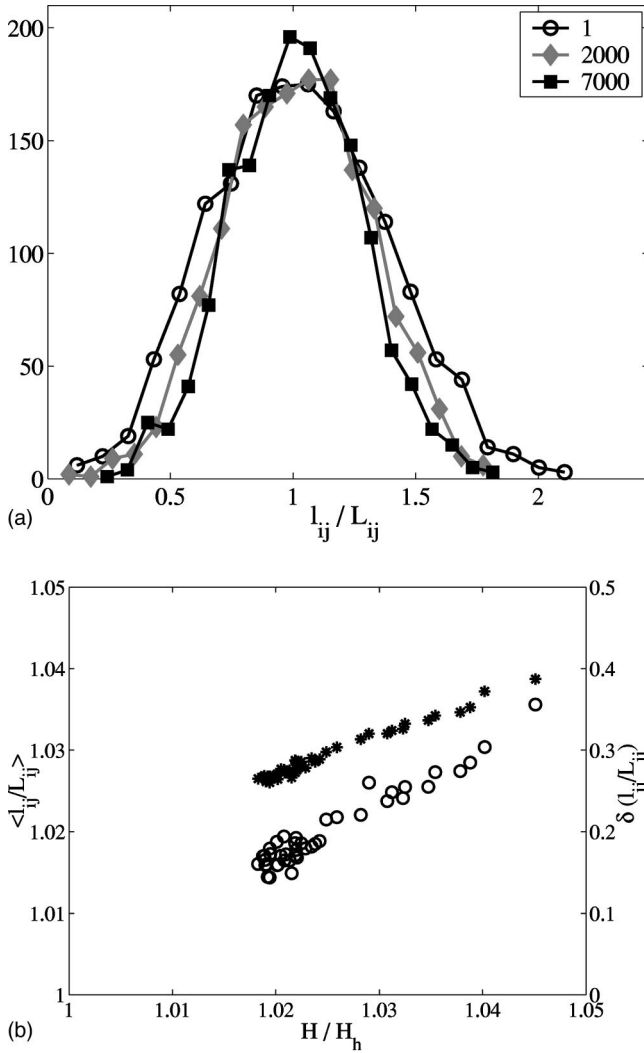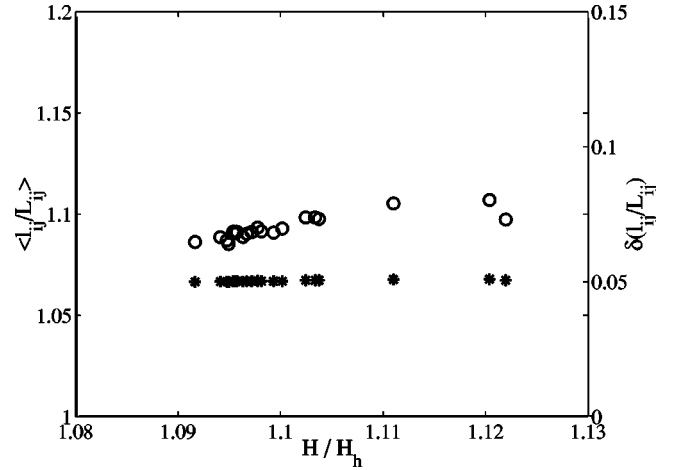

(b)

FIG. 5. Relaxation of simulated foams. (a) Ratio l_{ij}/L_{ij} between each edge's actual and reference lengths. Histograms are shown for the same foam before (1 MCS), during (2000 MCS), and at the end (7000 MCS) of the relaxation. (b) Average $\langle l_{ij}/L_{ij} \rangle$ (circles, left ordinate) and standard deviation $\delta(l_{ij}/L_{ij})$ (stars, right ordinate) during relaxation, plotted against the rescaled energy H/H_h.

C. Testing optimal edge length

We can measure both H_h and L_{ij} directly on a foam image simply by measuring all bubble areas [24]. In a distorted FFF [Fig. 1(b)], the edge lengths, bubble elongation, and bubble topologies all vary widely. Figure 4 presents the standard deviation from the mean, $\delta(l_{ij}/L_{ij})$ as a function of the rescaled energy H/H_h, for foam relaxations shown in Fig. 1(b). The abscissa and ordinate, reflecting *global* and *local* equilibration, show the same trend.

In simulated foams, we computed l_{ij}/L_{ij} for a foam during a relaxation from a distorted high energy state: the lower the energy, the narrower the histograms of l_{ij}/L_{ij} [Fig. 5(a)]. The mean value $\langle l_{ij}/L_{ij} \rangle$ decreases toward 1, and so does the standard deviation $\delta(l_{ij}/L_{ij})$, as the foam equilibrates [Fig. 5(b)]. At equilibrium, L_{ij} is statistically a good reference for l_{ij}. However, locally, l_{ij} differs from L_{ij}. The standard deviation $\delta(l_{ij}/L_{ij})$ reflects this local deviation, and thus the distance to the ground state [Fig. 5(b)].

We tested that the mean and the standard deviation of l_{ij}/L_{ij} are lower for equilibrated foams (Fig. 6) than for

impossible to calculate analytically for large N. However, a ''reference'' length is useful. For bubbles far from the foam boundaries and for a small area mismatch $\epsilon = (A_i - A_j)/(A_i + A_j) \ll 1$, we will assume that A_i and A_j alone determine an *optimal edge length* L_{ij}, and that, when the foam is in its ground state, l_{ij} is close to L_{ij}.

Statistically, in an equilibrium state (not the ground state) we expect that on average l_{ij} is close to L_{ij}, i.e., $\langle l_{ij}/L_{ij} \rangle$ is close to 1, where $\langle \rangle$ denotes averaging over the whole foam. However, individual l_{ij} could differ from the reference length L_{ij}, namely, the variance $\delta(l_{ij}/L_{ij})$ is not zero (for 3D foams, we might define similarly a characteristic size scale for faces and edges; the variance may be very large). Moreover, if under an extensional stress an incompressible foam is compressed in one direction and extended in the perpendicular direction, the edges parallel to the extension tend to be larger than their L_{ij}, while the edges parallel to

relaxing foams (Fig. 5). By coarsening a foam from a honeycomb structure, we gradually increase the area disorder while keeping the topology the same, i.e., in the early stage of coarsening. The area polydispersity affects H/H_h (since H is roughly the same for all foams [30] and H_h decreases when area polydispersity increases), but has virtually no effect on $\langle l_{ij}/L_{ij} \rangle$ nor on $\delta(l_{ij}/L_{ij})$, except for a (linear) increase smaller than 1%.

In the small-disorder limit, this treatment of area disorder allows us to predict the minimal energy configuration: the sorted pattern. The optimal edge length L_{ij} provides a *local* reference of how far the foam is from its equilibrium and thus opens the possibility of defining local strain in foams. We now consider the energy cost due to the topological disorder. Again, we consider only the weak disorder limit.

IV. TOPOLOGICAL DISORDER AND ELECTROSTATIC ANALOGY

The ''topological charge'' quantifies the deviation from a hexagonal lattice: an n-sided bubble has a charge $q \propto (6 - n)$. Charge is additive: the charge of a collection of bubbles is the sum of their individual charges [31]. A foam with periodic boundary conditions has zero total charge and hence an average of six sides per bubble [32].

The proportionality constant in the definition of q is arbitrary and cannot affect the physics. The literature employs both ± 1. For the convenience of the analogy with curvature as well as the electrostatic analogy below, we require that [33]:

$$q \equiv (6 - n)\frac{\pi}{3} = 2\pi - \frac{n\pi}{3}. \quad (9)$$

A. Geometrical Gauss-Bonnet theorem

Consider the ith bubble of a foam, and circle once counterclockwise around it. The tangent vector $\hat{t}$ along the bubble edge, which travels around the bubble once counterclockwise, rotates by 2π. Each side ij is an arc of length l_{ij} and of curvature κ_{ij}, and thus contributes $\kappa_{ij}l_{ij}$ to this rotation, while each vertex rotates the tangent vector $\hat{t}$ by $\pi/3$. The Gauss-Bonnet theorem links the average curvature of a bubble to its number of sides [34]:

$$\sum_j \kappa_{ij}l_{ij} = (6 - n_i)\pi/3 = q_i, \quad (10)$$

displaying how the topology constrains the curvature: five-sided bubbles are convex and seven-sided concave.
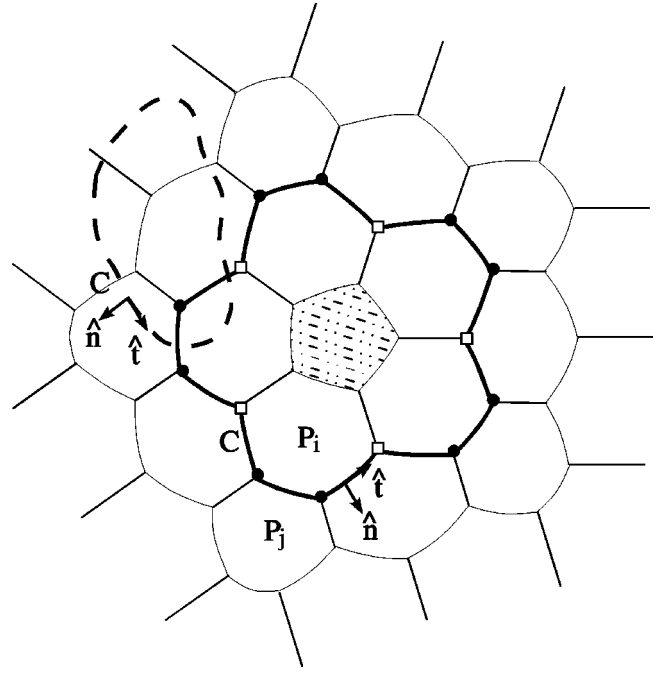

FIG. 7. A schematic of a 2D foam. The black contour C follows bubble edges and encloses a charge Q ($Q = \pi/3$ due to the pentagon). Vertices with squares point inward ($v_- = 5$) and vertices with circular disks point outward ($v_+ = 10$). The dashed contour C crosses bubble edges transversely. Along the contours tangent $\hat{t}$ and normal $\hat{n}$ vectors (arrows) are defined by the right-hand rule.

We now consider a contour C that follows only bubble edges and encloses a few bubbles. Aste, Boosé, and Rivier [31] define the number of vertices that originate an outward (inward) pointing edge as v^+ (v^-) (Fig. 7); e.g., $v^+ = 0$ if C is the boundary of the total foam, $v^- = 0$ if C encloses a single bubble. The *topological* Gauss-Bonnet theorem [31] states that C encloses a total topological charge Q:

$$Q(C) = \sum_{k \in C} q_k = (6 - v^+ + v^-)\frac{\pi}{3}, \quad (11)$$

where k labels the bubbles enclosed by C, and $Q(C)$ is their total charge.

Combining Eqs. (10) and (11), we can now write the *geometrical* Gauss-Bonnet theorem for a closed contour C that follows the bubble edges ij:

$$\sum_C \kappa_{ij}l_{ij} = Q(C) = \sum_{k \in C} q_k. \quad (12)$$

TABLE I. Proposed analogy between foams and electrostatics in two dimensions.

	Potential	Field	Charge
2D electrostatics	potential V	electric field $-\vec{\nabla}V$	electric charge e
2D foams	pressure P	curvature $\propto -\vec{\nabla}P$	topological charge $(6-n)\pi/3$

This theorem establishes the relation between a foam's topology (charges) and geometry (curvature). We now link them with the energy through an analogy to electrostatics.

B. Electrostatic analogy

Since κ is the spatial gradient of the pressure [Laplace's law, Eq. (3)], we can assimilate the pressure to an electrostatic potential and the topological charge to an electrostatic charge. In this analogy (Table I), each bubble represents a conducting platelet bearing a charge $q=(6-n)\pi/3$ distributed along its edges, which is uniform at equilibrium because the charge density is proportional to the the curvature. The edges are a thin layer of insulating material of thickness proportional to fluid fraction ϕ, which bear a large gradient of pressure (almost a discontinuity). Since we are not interested in the actual pressure within these thin edges, we choose to interpolate the pressure in such a way that $\Delta P=0$ within edges, and introduce the notation $\vec{E}\equiv-\vec{\nabla}P$:

$$\vec{E}=\epsilon_d\kappa\hat{n} \quad \text{(edges)},$$
$$\vec{E}=0 \quad \text{(bubbles)},$$

(13)

where $\epsilon_d=\phi L/\gamma$ is the edge's dielectric constant, κ its curvature, and $\hat{n}$ its outward normal.

This analogy holds if the fluid fraction ϕ is small enough that we can interpolate P within the Plateau borders. All physical quantities such as P, κ, or the energy defined below have a finite limit when $\phi\to0$: only notional quantities such as ϵ_r or $\vec{E}$ diverge. If the unit vectors $\hat{n}$, $\hat{t}$ are the normal and the tangent to C, respectively, as drawn in Fig. 7, Eqs. (4) and (12) become

$$\oint \vec{E}\cdot\hat{n}dl=\frac{Q}{\epsilon_d},$$
$$\oint \vec{E}\cdot\hat{t}dl=0.$$

(14)

These relations hold for *any contour C* (not necessarily parallel or perpendicular to edges) in the $\phi\ll1$ limit.

Equations (14) make the analogy to electrostatics obvious. Although both equations (14) look similar, they are physically different, describing, respectively, an outward flux through C (which, in 2D, is a line integral instead of a surface integral) and a circulation along C. Generalization to 3D cannot be exact, since the pressure and topology correlate with mean and Gaussian curvatures, respectively, which in general are independent quantities. However, numerical [35] and experimental [36,37] observations of a 3D growth law suggest a correlation between the mean and Gaussian curvatures, which means that an approximate analogy may hold in 3D.

C. Pressure field created by a topological charge

A positive q corresponds to a local high pressure. In turn the pressure gradient correlates with the bubbles' concavity.

For illustration, we consider a foam with all bubbles having the same area A, as in Fig. 7. Take one single ''defect'' bubble with a topological charge $q=(6-n)\pi/3$ as a germ bubble (dislocation), for instance, a regular pentagon. Construct around it a shell structure made of hexagons only: shell 0 is the germ bubble, bubbles of shell s are neighbors of bubbles of shell $s-1$. On Fig. 7, contour C encloses the first shell of bubbles. Since the pentagon is the single topological charge in this schematic foam, the hexagons surrounding the pentagon all have the same pressure. More generally, all bubbles of the same shell have the same pressure, namely, the pressure field is radial. All radial edges are straight, while the nonradial edges have a curvature, which we can calculate as follows.

Around the contour C that encloses the shell s, the numbers of vertices pointing inward, v^-, and outward, v^+, are equal to the numbers N_s and N_{s+1} of bubbles in shells s and $s+1$, respectively. Since the total charge within C is due only to the central topological defect, $q=\pi/3$, the Gauss-Bonnet theorem yields a recursive relation for N_s [31]:

$$N_s=N_{s-1}+n=sn.$$

(15)

Thus the number of bubble edges that C runs along is equal to $v^-+v^+=(2s+1)n$, their lengths all close to that of a regular hexagon, $L=3.72\sqrt{A}/6$. All these edges have the same curvature $\kappa(s)=[P(s)-P(s-1)]/\gamma$ determined by the pressure difference between the shells. Thus Eq. (12) yields approximately

$$(2s-1)nL\kappa(s)\approx q,$$

$$P(s)-P(s-1)=\gamma\kappa(s)\approx\frac{\gamma q}{(2s-1)nL}.$$

(16)

When the foam is sufficiently large, $s\gg1$, the asymptotic limits of both κ and P are easily determined:

$$\kappa(s)\propto\frac{q}{Ls},$$

$$P=\gamma\sum_s \kappa(s)\propto-\frac{\gamma q}{L}\ln s+P_0.$$

(17)

Here P_0 is a constant, the pressure P_b at the foam's boundary, and P grows logarithmically with the foam size as is characteristic of 2D electrostatics. Note that the pressure depends on the topological distance s rather than actual Euclidean distance.

D. Topological energy cost

In a honeycomb, when a topological defect induces a curvature in the neighboring edges, the total foam perimeter increases. To estimate this increase, consider two vertices separated by a distance a. An arc with curvature κ connecting them has a length $l=2\alpha/\kappa$, where $\alpha=\arcsin(a\kappa/2)$ is half of the subtended angle. The difference between a and l is the length increase due to the curvature:

$$l - a = l\left(\frac{\kappa^2 l^2}{24} + O(\kappa^4 l^4)\right). \tag{18}$$

As expected, $l - a$ is positive and quadratic in κ. By summing over all edges of the foam, and keeping only the leading order when $\kappa l \ll 1$, we obtain the increase in energy due to curvature:

$$H_t \approx \gamma \sum_{i < j} l_{ij} \times \frac{\kappa_{ij}^2 l_{ij}^2}{24}. \tag{19}$$

For instance, around the single topological charge, $\kappa(s)$ decreases as q/s [Eq. (17)]. The summation over all curved edges yields the energy cost due to this single topological defect:

$$H_t \approx \gamma \sum_s (2s-1)nL \times \frac{q^2}{24(2s-1)^2 n^2}$$

$$= \frac{\gamma L q^2}{24n} \sum_s \frac{1}{2s-1}. \tag{20}$$

It grows logarithmically with the size of the foam, as expected in analogy with the self-energy of a 2D electrostatic charge. For a large foam, a single topological charge costs so much energy that it never occurs in real foams.

E. Several topological charges

Consider two charges q, q' separated by a (topological) distance $s \gg L$; the interaction energy varies as

$$H_t \sim -qq' \gamma L \ln\left(\frac{s}{L}\right). \tag{21}$$

It decreases when charges of like sign separate or charges of unlike sign aggregate. For instance, in Fig. 1(a), the heptagon (indicated by a number 7) has two pentagonal neighbors. This ''effective interaction'' of topological origin, which previous work has assumed or derived empirically [14], has important consequences. For instance, this interaction explains the origin of the correlations between bubbles: the side number distribution and the Aboav-Weaire law [38].

We can extend our electrostatics vocabulary. Two opposite charges $-q + q$ [e.g., a pentagon-heptagon pair, Fig. 2(b)] a distance $d \sim L$ apart constitute a dipole of moment $\vec{p} = q\vec{d}$, which deforms neighboring bubbles and induces curved edges in the hexagons around it. At a distance $s \gg d$ away from this dipole, the pressure varies as $1/s$ and the curvature as $1/s^2$, similar to the dipolar potential in 2D. A dipole can pair with another dipole [Fig. 2(b)] to form a topological quadrupole [Fig. 2(c)], which affects the honeycomb lattice over a much shorter range, the pressure varying as $1/s^2$ and the curvature as $1/s^3$. Note that a T1 process conserves not only the total charge but also the total dipolar moment, altering only the foam's quadrupolar moment: it is a current of dipoles.

This description remains valid even for many charges, as long as the curvature fields they induce are small and can be added by linear superposition. The pressure fields of multiple charges are added linearly too. However, the present calculations assume equal areas; they become more difficult when the area disorder couples with the topological disorder. Physically, H_t is minimal when the foam is as neutral (charge-free) as possible, with the lowest concentration of isolated charges or dipoles compatible with its other topological constraints, such as boundary conditions.

V. BOUNDARY CONDITIONS

The possible boundary conditions for foam are free if the foam is surrounded by a fluid medium, Fig. 1(a); periodic, Fig. 2(b); fixed if it touches a solid box, Fig. 2(d); or some combination of these three, Fig. 2(a). As already mentioned we use the word ''boundary'' strictly as the external limit of a foam, while ''edge'' is the thin fluid line between two bubbles.

A. Total charge of a foam

Periodic boundary conditions guarantee that the total charge $Q = 0$ [32]. For all other boundary conditions, we can apply the topological Gauss-Bonnet theorem [31] to the boundary of the foam: the number of vertices pointing outward is $v_+ = 0$ and the number of vertices pointing inward is $v_- = N_b$ [39]. The total charge of a foam is then $Q = (N_b + 6)\pi/3$. This is checked in Fig. 1(a) by visual inspection: there are $N_b = 19$ bubbles at the free boundary and a total topological charge $Q = 25\pi/3 = 26.2$. Moreover, for this foam $\sum_i \kappa_{0i} l_{0i} = 26.5 \pm 3.8$, in good agreement with Eq. (12) despite a rather large imprecision in our curvature measurements.

Introducing a modified definition $\tilde{q}$ for charges at the boundary is more convenient (see below):

$$\tilde{q} = (6-n)\frac{\pi}{3} \equiv q \quad \text{(bulk)}, \tag{22}$$

$$\tilde{q} = (5-n)\frac{\pi}{3} \quad \text{(boundary)}. \tag{23}$$

With this new definition, the total charge of a foam becomes simply $\tilde{Q} = \sum_i \tilde{q}_i = 2\pi$.

B. Topology uniquely determines pressure and curvature

For a free foam, the outer fluid fixes the pressures at the foam boundary. A fixed boundary, on the other hand, requires that the gradient $-\vec{E}$ of P (perpendicular to each bubble edge, itself perpendicular to the boundary [40,41]) is parallel to the boundary. Thus, in these two cases, the topological charges determine the pressure in the foam as a Dirichlet or a Neumann problem, respectively. Therefore, the pressure field should probably be *unique* for fixed topology.

The pressures and areas in turn fix the energy. We illustrate this for a foam with free boundaries, through the relation derived from the Laplace law which expresses the foam's mechanical equilibrium [42]:
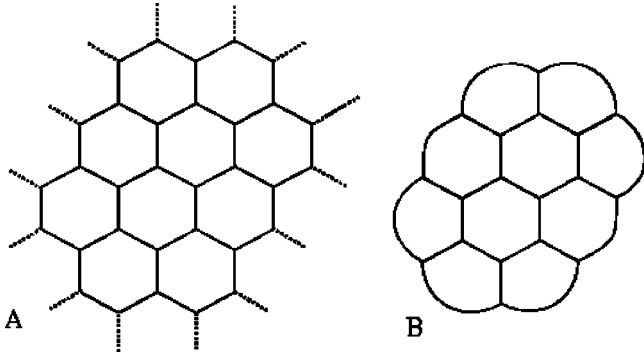
FIG. 8. Difference between an infinite foam and a finite foam with free boundary conditions. (a) Part of an infinite hexagonal foam enclosed by a contour. (b) Schematic picture of the same bubble cluster with a free boundary, the straight edges at the boundary relaxed to circular arcs.

$$H = 2 \sum_{i=1}^{N} P_i A_i - 2 P_b \sum_{i=1}^{N} A_i, \qquad (24)$$

where P_b is the pressure of the outer fluid at the foam's boundary. The energy reaches its minimum when the largest bubbles have as low a pressure as possible. Equation (24) can be generalized to D dimensions, H being now the hypersurface energy, and A the hypervolume:

$$H = \frac{D}{D-1} \sum_{i=1}^{N} (P_i - P_b) A_i. \qquad (25)$$

C. Fixed boundaries: Topological constraints

As mentioned above, for fixed boundary conditions [Fig. 2(d)] bubble edges are perpendicular to the boundaries [40]. The Gauss-Bonnet theorem implies that the integral $\kappa_{ij} l_{ij}$ of edge curvatures, plus the $\pi/3$ turn at each of the $n-2$ vertices, plus two $\pi/2$ turns at the boundary, plus the curvature κ_{0i} of the boundary itself, add to 2π. This *boundary Gauss-Bonnet theorem* is

$$\sum_{j=1}^{N} \kappa_{ij} l_{ij} + (n_i - 2) \frac{\pi}{3} + 2 \frac{\pi}{2} + \kappa_{0i} l_{0i} = 2\pi. \qquad (26)$$

To emphasize the physical meaning of $\tilde{q}$, we rewrite it as

$$\sum_{j=1}^{N} \kappa_{ij} l_{ij} = \tilde{q}_i + \kappa_{0i} l_{0i}. \qquad (27)$$

At a straight boundary $\kappa_{0i} = 0$; a pentagon $\tilde{q}_i = 0$ can have all straight edges, while a hexagon $\tilde{q}_i \neq 0$ cannot, hence $\tilde{q}$ is more relevant than q. A curved boundary has the same effect as a small topological charge $\kappa_{0i} l_{0i} \neq 0$. By the Gauss-Bonnet theorem along the boundary, the solid box imposes a total charge

$$\tilde{Q} = \sum_{i} \kappa_{0i} l_{0i} = 2\pi. \qquad (28)$$

The shape of the solid box determines the distribution of the total charge $\tilde{Q} = 2\pi$ among the bubbles touching the boundary: the $\kappa_{0i} l_{0i}$'s act as a line distribution of charges along the boundary. If the solid box has all corner angles a multiple of $\pi/3$, we can have the $\tilde{q}$'s be multiples of $\pi/3$, compatible with all bubble edges being straight. In general, however, the solid box imposes $\tilde{q}$'s that are not multiples of $\pi/3$, resulting in curved bubble edges. The same applies to a concave boundary, for instance, an obstacle placed in the middle of the foam, which introduces a total charge $\tilde{Q} = -2\pi$, as can be visually checked in Fig. 2(d).

D. Free boundary: Contribution to the energy

The energy contribution from the boundary conditions, H_b, is a function of the number of bubbles at the boundary, N_b. Take an infinite foam, and consider in it a contour C enclosing a finite number of bubbles N. The perimeter of this contour is $\mathcal{L}_C$, contributing $\mathcal{L}_C/2$ to H. If we take the part of the foam enclosed by C and give it a free boundary, the straight boundary edges relax and reach a new perimeter $\mathcal{L}_b$, as Fig. 8 shows. The new perimeter is slightly smaller than $\mathcal{L}_C$, but Eq. (1) now counts it twice, contributing $\gamma \mathcal{L}_b$ to H. The cost due to the free boundary is thus the difference between the two terms:

$$H_b = \gamma \left(\mathcal{L}_b - \frac{\mathcal{L}_C}{2} \right). \qquad (29)$$

H_b is always positive and grows like N_b: for a given N, it reaches its minimum for $N_b \sim \sqrt{N}$, i.e., for a rather round boundary. H_b is of order $\gamma \mathcal{L}_C/2$ and is difficult to evaluate in general, since the shape relaxation is nontrivial.

We study a special case for insight: an "isobaric" foam in which all bubbles have (exactly or approximately) the same pressure $P_i = P$, with a large number of bubbles N and free boundaries. In this case all internal edges are straight and all boundary edges have the same curvature $\kappa_b = (P - P_b)/\gamma$. Equation (24) gives the total foam energy

$$H = 2(P - P_b) \sum_{i=1}^{N} A_i = 2\gamma \kappa_b N \bar{A}. \qquad (30)$$

H has the same value as if all bubbles had the area $A_i = \bar{A}$ [30]: for N large enough that $N \gg N_b$, boundary effects are much smaller than H, which varies as $H \to 3.72 N(\gamma/2)\sqrt{\bar{A}}$; hence in the large-$N$ limit

$$\kappa_b \approx \frac{3.72}{4\sqrt{\bar{A}}} + O\left(\frac{N_b}{N} \right). \qquad (31)$$

Thus κ_b is about half the curvature $\sqrt{\pi/A}$ of a single round bubble. The FFF in Fig. 1(a) obeys this relation with a 15% error because κ_b is not uniform. This result generalizes to any dimension D, with $\bar{L}$ and $\bar{A}$ the average hyperarea and hypervolume

$$\kappa_b = \frac{(D-1)\bar{L}}{2D\bar{A}}\left[1 + O\left(\frac{N_b}{N}\right)\right], \qquad (32)$$

which determines the difference between $\mathcal{L}_C$ and $\mathcal{L}_b$, the perimeters of the contour in the foam and the free boundary.

The energy cost due to the boundary, H_b, can be better estimated for a 2D honeycomb. In a honeycomb, C contains $v_+ + v_- = 2N_b + 6$ straight edges of length $L = 3.72\sqrt{A}/6$; hence $\mathcal{L}_C = (2N_b + 6)L$. After the boundary is created, the topological charge of the finite foam is $Q = (N_b + 6)\pi/3$, and Eq. (12) relates $\mathcal{L}_b$ to κ_b:

$$\kappa_b \mathcal{L}_b = \frac{\pi}{3}(N_b + 6). \qquad (33)$$

Equations (29), (30), and (33) are now closed; we can calculate H_b, κ, and $\mathcal{L}_b$ explicitly. They are particularly simple in the limit of a large foam $N \gg N_b \gg 1$, where, up to $O(1/N_b)$ and $O(N_b/N)$ terms,

$$H_b = \gamma\left(\frac{\pi}{3}\frac{N_b}{\kappa_b} - N_b L\right)$$

$$\approx \gamma N_b L\left(2\frac{\pi}{3.46} - 1\right). \qquad (34)$$

The factor 2 reflects the creation of a boundary; the ratio between π and $(3.72)^2/4 = 2\sqrt{3} = 3.46$ reflects the relaxation of regular hexagons into circular arcs.

VI. SUMMARY

Foam structures are the result of surface energy minimization. Most foam studies have focused on a few consequences of the energy minimization and ignored the foam energy itself. We reconsider the equilibrium energy of 2D foams with given bubble areas and draw from it the general understanding of foam structure as natural results of energy minimization.

The pressure P, edge curvature κ, and topological charge $q = (6 - n)\pi/3$ are good variables to characterize a foam. They present a profound analogy with 2D electrostatic potential, field, and charge, respectively, through the geometrical Gauss-Bonnet theorem [Eq. (12)]. The analogy relates the curvature, topology, and energy of a foam; indicates that the topology determines a foam's energy; and explains the origin of topological and geometrical correlations in foams.

We have defined reference values H_h and L for the foam's total energy H and edge length l; both can be directly measured on an image. The zeroth-order estimate of the ground energy H_h is a function of the area distribution only, independent of the topology. The estimate of the edge length in the ground state, L, is a function only of the areas of two bubbles sharing the edge. The ratios H/H_h and l/L provide global and local markers, respectively, of how far a foam is from its ground state, opening the way toward an intrinsic definition of strain in a foam [29].

The present analysis also provides insight into the classic minimum perimeter problem generalized to nontrivial situa-

TABLE II. Elongation $e(n) = \mathcal{L}/\sqrt{A}$ of regular bubbles with n curved edges meeting at $2\pi/3$ angles.

n	$e(n)$
2	3.779410
3	3.742190
4	3.730802
5	3.725462
6	$3.722420 = 2^{3/2}3^{1/4}$
7	3.720471
8	3.719130
9	3.718151
10	3.717409
20	3.714489
50	3.713052
∞	$3.712219 = 2(\pi)^{3/2}/3$

tions: large number of bubbles, arbitrary area distributions, and various boundary conditions. It explains physically the different contributions to a foam's energy (area mismatch, topology, and boundaries) and predicts the foam configurations corresponding to their ground state (hexagons sort according to their size; topological charges of the same sign tend to separate and opposite signs tend to aggregate).

This analysis applies to any perimeter-minimizing material, where the energy is an increasing function of the total bubble perimeter. The analysis does not depend on the characteristic size and energy scales. It is also valid for foams in which bubble areas vary slowly. Deriving approximate results for 3D seems possible.

APPENDIX: CONJECTURES REGARDING THE MINIMAL PERIMETER PROBLEM

We consider a foam with all bubbles areas A_i given. Their topology is free to vary (each bubble remains connected). Their shape is free to vary too; each bubble has an elongation defined as

$$e_i = \frac{\mathcal{L}_i}{\sqrt{A_i}}. \qquad (A1)$$

The problem is to find the minimum value $\min(H)$ the foam energy could reach, i.e., to find

$$\min\left(\sum_i \mathcal{L}_i\right) = \min\left(\sum_i e_i\sqrt{A_i}\right). \qquad (A2)$$

While this problem is still open, we make a few conjectures and comments

a. Elongation of a regular bubble. Consider a bubble with n equal sides. They meet at $2\pi/3$ angles. Thus, due to the Gauss-Bonnet theorem, each edge turns an angle (i.e., subtends an angle) 2α, where $\alpha = \pi(1/n - 1/6)$. Some simple algebra shows that the bubble elongation $e(n)$ is

$$\frac{1}{e(n)^2} = \frac{1}{4n\alpha^2}\left(\alpha - \frac{\sin(\alpha)\sin(\pi/6)}{\sin(\pi/n)}\right). \qquad (A3)$$

b. The function $e(n)$ is almost constant. Table II shows a few values of $e(n)$. The function diverges when $n \to 1$, since no arc of a circle can self-intersect at a $2\pi/3$ angle. There is no limit when $n \to 0$: a circle is qualitatively different from all other bubbles. The function is regular at all $n > 1$, including at $n = 2$ and 6; although it decreases with n, it is surprisingly close to a constant: $e(2)$ is only 2% above $e(\infty)$.

c. Lower bound for the total perimeter. In a foam, each bubble tends to be as round as possible, subject to the constraints of its neighbors. Since all regular bubbles have $e > e(\infty) = 3.71$, we conjecture a lower bound not only for the elongation averaged over the foam,

$$\bar{e} > e(\infty) \approx 3.71, \qquad (A4)$$

but also for the total perimeter,

$$\sum_i \mathcal{L}_i > 3.71\sum_i \sqrt{A_i},$$
$$\langle\mathcal{L}_i\rangle > 3.71\langle\sqrt{A_i}\rangle. \qquad (A5)$$

d. Comments on this lower bound. We are not aware of any foam pattern violating this lower bound. Morgan [43] finds that an alternate tiling of eight-sided bubbles and 0.157 times smaller four-sided bubbles [take Fig. 2(a) of Ref. [2] and let curvatures relax] has $\bar{e} = 3.722\,418$ and $\langle P_i\rangle = 3.719\langle\sqrt{A_i}\rangle$, so Eqs. (A4) and (A5) still hold.

e. Estimate for a natural foam. In natural foams, bubbles with five, six, and seven sides dominate [15]. As a zeroth-order estimate, we conjecture that

$$\bar{e} \approx e(6) \approx 3.72, \qquad (A6)$$

and the minimum value of $\langle P_i\rangle/\langle\sqrt{A_i}\rangle$ is closer to $e(6) \approx 3.72$ than to $e(\infty) \approx 3.71$:

$$H_h \approx 3.72\frac{\gamma}{2}\sum_i \sqrt{A_i}, \qquad (A7)$$

where the subscript h stands for hexagons.

f. Comments on this estimate. In Morgan's above example [43], both $\bar{e}$ and $\langle P_i\rangle/\langle\sqrt{A_i}\rangle$ are lower than this value. On the other hand, when all areas are equal, the minimum (honeycomb lattice [1]) has of course $\bar{e} = \Sigma_i\mathcal{L}_i/\Sigma_i\sqrt{A_i} = e(6)$. For convex bubbles (i.e., with straight edges), it has been demonstrated that $\bar{e} \geq e(6)$ [44]. Finally, note that it is compatible with the fact that for convex hexagons (i.e., with straight edges) with $2\pi/3$ angles, $\Sigma_i\mathcal{L}_i$ is a function of $\Sigma_i A_i$ only [30].

[1] T. C. Hales, e-print xyz.lanl.gov/math.MG/9906042; see also Sci. News, Washington, DC **156**, 60 (1999); E. Klarreich, Am. Sci. **88**, 152 (2000).

[2] F. Morgan, Trans. Am. Math. Soc. **351**, 1753 (1999).

[3] R. Osserman, Bull. Am. Math. Soc. **84**, 1182 (1978).

[4] F. J. Almgren, Jr., Mem. Am. Math. Soc. **4**, 165 (1976); F. Morgan, *Geometric Measure Theory: A Beginner's Guide*, 3rd ed. (Academic Press, New York, July, 2000).

[5] F. J. Almgren, Jr. and J. E. Taylor, Sci. Am. July 1976, p. 82. See also J. E. Taylor, Ann. Math. **103**, 489 (1976).

[6] H. Howards, M. Hutchings, and F. Morgan, Am. Math. Monthly **106**, 430 (1999).

[7] F. Morgan, Pac. J. Math. **165**, 347 (1994); Am. Math. Monthly **101**, 343 (1994).

[8] J. Foisy, B.A. dissertation, Williams College, Williamstown, MA, 1991 (unpublished); J. Foisy, M. Alfaro, J. Brock, N. Hodges, and J. Zimba, Pac. J. Math. **159**, 47 (1993).

[9] C. Cox, L. Harrison, M. Hutchings, S. Kim, J. Light, and M. Tilton, Real Anal. Exch. **20**, 313 (1994/95).

[10] J. Sullivan, in *Foams and Emulsions*, Vol. E354 of *NATO Advanced Study Institute, Series E: Applied Sciences*, edited by J. F. Sadoc and N. Rivier (Kluwer, Dordrecht, 1999).

[11] D. Weaire and N. Rivier, Contemp. Phys. **25**, 59 (1984).

[12] J. A. Glazier, Ph.D. dissertation, University of Chicago, 1989 (unpublished).

[13] J. A. Glazier and D. Weaire, J. Phys.: Condens. Matter **4**, 1867 (1992).

[14] N. Rivier, in *Disorder and Granular Media*, edited by D. Bideau and A. Hansen (Elsevier, Amsterdam, 1993), pp. 55–102.

[15] J. Stavans, Rep. Prog. Phys. **56**, 733 (1993).

[16] *Foams and Emulsions* [Ref. [10].

[17] S. Hutzler and D. Weaire, *Physics of Foams* (Oxford University Press, Oxford, 1999).

[18] M. O. Magnasco, Philos. Mag. B **69**, 397 (1994).

[19] Y. Jiang, P. J. Swart, A. Saxena, M. Asipauskas, and J. A. Glazier, Phys. Rev. E **59**, 5819 (1999).

[20] If energy H is a strictly increasing function of the total perimeter $\mathcal{L} = \Sigma_{i=0}^N \mathcal{L}_i = \Sigma_{i,j=0}^N l_{ij}$, then the mechanical equilibrium (energy is extremal with respect to infinitesimal displacements, $dH = 0$) still follows as the Laplace law, with an effective surface tension $\gamma_{eff} = 2\,dH/d\mathcal{L} > 0$. In most foams, the amount of edge fluid is fixed: when the perimeter varies, the edge thickness varies too. Even if this variation changes γ_{eff}, the geometry of the pattern remains the same.

[21] F. Elias, C. Flament, J.-C. Bacri, O. Cardoso, and F. Graner, Phys. Rev. E **56**, 3310 (1997).

[22] F. Elias, C. Flament, J. A. Glazier, F. Graner, and Y. Jiang, Philos. Mag. B **79**, 729 (1999).

[23] E. Holm, J. A. Glazier, D. J. Srolovitz, and G. S. Grest, Phys. Rev. A **43**, 2662 (1991).

[24] We use the edge length $L(A)$ of a hexagon as a mean-field approximation. $L(A)$ is independent of the bubble topology and thus constant through a T1 and easy to measure on a picture. We are currently trying to relax this approximation to treat both area and topological disorder: as discussed in the Appendix, an n-sided bubble has a ''reference length'' $L(A,n) = e(n)\sqrt{A}/n \approx 3.72\sqrt{A}/n$.

[25] See, e.g., M. A. Herman and H. Sitter, *Molecular Beam Epitaxy*, Vol. 7 of *Springer Series in Material Science*, 2nd ed. (Springer, Berlin, 1996).

[26] If the area disorder were large, the topological disorder would be large, too: e.g., a binary area distribution, where tiny bubbles decorate the vertices of the large-bubble honeycomb lattice; Fig. 2(a) of Ref. [2].

[27] F. Elias, J.-C. Bacri, F.-H. de Mougins, and T. Spengler, Philos. Mag. Lett. **79**, 389 (1999).

[28] S. Alexander, Phys. Rep. **296**, 65 (1998).

[29] Y. Jiang, M. Asipauskas, J. A. Glazier, and F. Graner (unpublished).

[30] The total perimeter of a set of hexagons, possibly irregular, depends only on the sum of their areas, not on their detailed area distribution, as long as they have *straight* edges and $2\pi/3$ contact angles. See, for instance, I. M. Lipschitz, Zh. Éksp. Teor. Fiz. **42**, 1354 (1962) [Sov. Phys. JETP **15**, 939 (1962)] or S. A. Safran, Phys. Rev. Lett. **46**, 1581 (1981). In our notation, when the area polydispersity is increased at constant total area $\Sigma_i A_i$, H_h decreases, H_a increases, and $H_h + H_a$ is roughly constant if the edges remain nearly straight.

[31] T. Aste, D. Boosé, and N. Rivier, Phys. Rev. E **53**, 6181 (1996).

[32] This is usually derived from the Euler theorem [12,14], applied here to a non-simply-convex foam (e.g., on a torus).

[33] This definition can be generalized to a curved two-dimensional facet. If the contact angle between edges is θ ($\theta = 2\pi/3$ for a flat surface in 2D, $\theta = 109.7°$ for a face of a 3D bubble), the topological charge is $q \equiv 2\pi - n(\pi - \theta_D)$. Using the results of J. Avron and D. Levine, Phys. Rev. Lett. **69**, 208 (1992), one finds that q is the sum of the Gaussian curvature of the face and the curvature of the edge.

[34] J. von Neumann, in *Metal Interfaces* (American Society for Metals, Cleveland, 1952), pp. 108–110, quoted, e.g., in [12,13,15].

[35] J. A. Glazier, Phys. Rev. Lett. **70**, 2170 (1993).

[36] C. Monnereau and M. Vignes-Adler, Phys. Rev. Lett. **80**, 5228 (1998); C. Monnereau, N. Pittet, and D. Weaire, Europhys. Lett. (to be published).

[37] B. Prause and J. A. Glazier, Proceedings of the ''European 2000'' Conference, Delft, edited by P. Zitha (MIT Editions, in press).

[38] G. Schliecker and S. Klapp, Europhys. Lett. **48**, 122 (1999).

[39] Except, of course, in the trivial case of a single bubble where $v_- = 0 \neq N_b = 1$.

[40] G. Hruska, D. Leykekhman, D. Pinzon, B. Shoy, and J. Foisy, Rocky Mountain J. Math. (to be published).

[41] In the rare case where the edge fluid does not wet the box boundaries, e.g., Fig. 1(b), the edges are tangent to the boundaries. Removing these edges leads to an incomplete foam with edges meeting the boundary perpendicularly.

[42] S. Ross, Ind. Eng. Chem. **61**, 48 (1969) (with references to P. G. Tait in the 1860s); H. Aref and D. Vainshtein, Phys. Fluids **12**, 28 (2000). We independently suggested the following equivalent but shorter demonstration based on a Legendre transformation, using P_b as a Lagrange multiplier. Consider a free foam with *fixed pressures*, not areas. At equilibrium, the enthalpy $\mathcal{H} \equiv H - \Sigma_{i=1}^{N}(P_i - P_b)A_i$ is extremal. Thus, under dilation, $L \to \lambda^{D-1}L$, $A \to \lambda^D A$, $\mathcal{H}(\lambda) = \lambda^{D-1}H - \lambda^D \Sigma_{i=1}^{N}(P_i - P_b)A_i$ is extremal at $\lambda = 1$.

[43] F. Morgan (personal communication).

[44] L. Fejes Tóth, *Lagerungen in der Ebene, auf der Kugel und im Raum*, Vol. 65 of *Die Grundlehren der Math. Wiss.* (Springer, Berlin, 1972), p. 84.